

Study of Heat Transfer Characteristics of Bent Heat Pipe with Multiple Heat Sources by Using Finite Element Method

Nampon Sangpab¹, Phrut Sakulchangsattajai¹, Niti Kammuang-lue¹, Pradit Terdtoon¹

Received: 15 June 2015; Accepted: 13 July 2015

Abstract

Incompressible flow simulation of bent heat pipes with multiple heat sources at steady state is presented in this paper. The thermal performance was simulated in two dimension to predict the distribution of temperature, velocity and pressure in heat pipes. The fluid flow and heat transfer are determined from continuity, Navier-Stokes, and energy equations and they were analyzed by using Finite Element Method (FEM). The results from simulation of heat pipes have been compared to the experiments data from other researchers.

Keywords: finite element method, heat pipe, simulation

Introduction

Heat pipe is a heat transfer device that combines the principles of both thermal conductivity and phase transition to efficiently manage the transfer of heat between two solid interfaces. Heat pipes are widely used for thermal management in laptop and other applications. Heat sources from a CPU chip and VGA card is rapidly transferred to a heat sink via heat pipe. To decrease weight and size of laptop. Heat pipe must occupy less space in laptop. Tube bending is an unavoidable process and a heat pipe must uses with multiple heat sources to reduce the space in laptop. As in other applications, shape of heat pipe must be varied. Many researchers have developed similar heat pipes²⁻⁴. Most of them studied straight shape of heat pipe with one heat source and having a few simulations that use finite element method. Finite element method can be used in any shape so this

work will study bent heat pipes with multiple heat sources. In this study, simulation of heat pipe operation will simulate fluid flow and heat transfer of a bent heat pipe with multiple heat sources. The governing equations and boundary conditions were solved by using finite element method.

Governing Equations

The heat pipe domains consist of 3 parts: First is the vapor of working fluid in the vapor core. Second is the liquid of the working fluid in the wick. Last is the wall of the container. Under normal operation, the working fluid in the evaporator section transformed into a vapor, which flows to the condenser section. Working fluid in vapor phase subsequently condensed to a liquid, and returned back to the evaporator section through capillary forces in the wick.

¹ Department of Mechanical Engineering, Faculty of Engineering Chiang Mai University, Chiang Mai, Thailand 50200.
Email: nampon.s@hotmail.com

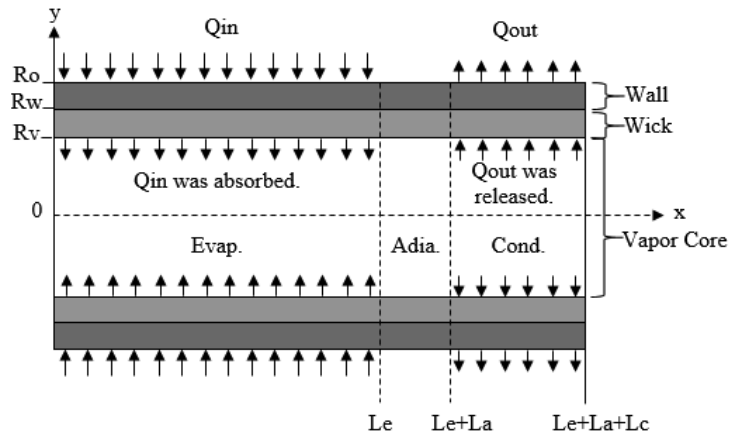


Figure 1 The schematic diagram of the heat pipe and the coordinate system.

In this simulation, Heat transfer and fluid flow were assumed to be incompressible flow, laminar flow and steady state.

1. Governing equations in vapor core

Continuity equation

$$\frac{\partial u_v}{\partial x} + \frac{\partial v_v}{\partial y} = 0 \tag{1}$$

Navier-Stokes equation

$$\rho_v \left(u_v \frac{\partial u_v}{\partial x} + v_v \frac{\partial u_v}{\partial y} \right) = -\frac{\partial p_v}{\partial x} + 2\mu_v \frac{\partial^2 u_v}{\partial y^2} + \mu_v \left(\frac{\partial^2 u_v}{\partial y^2} + \frac{\partial^2 v_v}{\partial x \partial y} \right) \tag{2}$$

$$\rho_v \left(u_v \frac{\partial v_v}{\partial x} + v_v \frac{\partial v_v}{\partial y} \right) = -\frac{\partial p_v}{\partial y} + 2\mu_v \frac{\partial^2 v_v}{\partial y^2} + \mu_v \left(\frac{\partial^2 u_v}{\partial x \partial y} + \frac{\partial^2 v_v}{\partial x^2} \right) \tag{3}$$

Energy equation

$$\rho_v c_{v,v} \left(u_v \frac{\partial T_v}{\partial x} + v_v \frac{\partial T_v}{\partial y} \right) = k_v \left[\frac{\partial^2 T_v}{\partial x^2} + \frac{\partial^2 T_v}{\partial y^2} \right] \tag{4}$$

2. Governing equations in wick

The governing equation in vapor core was defined as follows. The Darcy's law was apply to momentum equation.

Continuity equation

$$\frac{\partial u_l}{\partial x} + \frac{\partial v_l}{\partial y} = 0 \tag{5}$$

Navier-Stokes equation

$$\rho_l \left(u_l \frac{\partial u_l}{\partial x} + v_l \frac{\partial u_l}{\partial y} \right) = -\frac{\partial p_l}{\partial x} + 2\mu_l \frac{\partial^2 u_l}{\partial y^2} + \mu_l \left(\frac{\partial^2 u_l}{\partial y^2} + \frac{\partial^2 v_l}{\partial x \partial y} \right) - \frac{\mu_l u_l \varepsilon}{K} \tag{6}$$

$$\rho_l \left(u_l \frac{\partial v_l}{\partial x} + v_l \frac{\partial v_l}{\partial y} \right) = -\frac{\partial p_l}{\partial y} + 2\mu_l \frac{\partial^2 v_l}{\partial y^2} + \mu_l \left(\frac{\partial^2 u_l}{\partial x \partial y} + \frac{\partial^2 v_l}{\partial x^2} \right) - \frac{\mu_l u_l \varepsilon}{K} \tag{7}$$

Energy equation

$$\rho_l c_{p,l} \left(u_l \frac{\partial T_l}{\partial x} + v_l \frac{\partial T_l}{\partial y} \right) = k_{eff} \left[\frac{\partial^2 T_l}{\partial x^2} + \frac{\partial^2 T_l}{\partial y^2} \right] \tag{8}$$

3. Governing equations in container wall

The energy equation in the wall is the steady heat conduction equation as follows.

$$\frac{\partial^2 T_s}{\partial x^2} + \frac{\partial^2 T_s}{\partial y^2} = 0 \tag{9}$$

Boundary Conditions

The boundary conditions at both pipe ends are;

$$x = 0; \quad u_v = v_v = u_l = v_l = \frac{\partial T_v}{\partial x} = \frac{\partial T_l}{\partial x} = \frac{\partial T_s}{\partial x} = 0, \quad P_v = P_{ref} = 20.51 \text{ kPa}, \quad T_v = T_{ref} = 333.15 \text{ K}$$

$$x = L; \quad u_v = v_v = u_l = v_l = \frac{\partial T_v}{\partial x} = \frac{\partial T_l}{\partial x} = \frac{\partial T_s}{\partial x} = 0, \quad P_v = P_l$$

The boundary conditions at centerline are;

$$y = 0; \quad u_v = 0, \quad P_v = P_{sat}, \quad T_v = T_l = T_{sat}(P_v)$$

$$\rho_v v_v = \rho_l v_l = \begin{cases} -\frac{Q}{2\pi R_v L_e h_{fg}} \\ +\frac{Q}{2\pi R_v L_c h_{fg}} \end{cases}$$

The boundary conditions at liquid-wall interface are;

$$y = R_w; \quad u_v = v_v = u_l = v_l = 0$$

The boundary conditions at outer wall are;

$$y = R_o; \quad \frac{\partial T_s}{\partial y} = \begin{cases} -\frac{Q}{k_s 2\pi R_o L_e} \\ -\frac{Q}{k_s 2\pi R_o L_c} \end{cases}$$

Materials and Methods

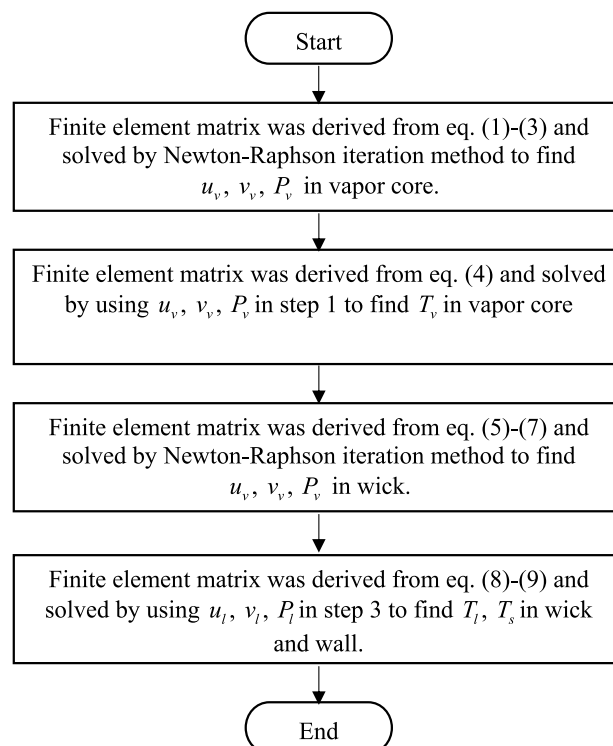


Figure 2 Flow diagram of methodology.

The methodology procedure is illustrated in (Figure 2). The conservation equations and boundary conditions were solved using the finite element method that matrices were derived by using the standard Galerkin approach and used the six-node triangle element. The velocity and pressure distributions in the vapor core were calculated from the equation of continuity and the momentum equations, Eqs. (1) - (3). Next, the temperature distribution in the vapor core was calculated from the energy equation, Eq. (4). The velocity and pressure distributions of liquid in wick were calculated from the equation of continuity and the momentum equations, Eqs. (5), (6), (7). Finally, the temperature distribution of the wick and the wall of container were calculated from the energy equations, Eqs. (8) and (9).

Result and Discussions

To verify this simulation, the results from this simulation were compared with the simulation from N. Thuchayapong¹. The specifications of bend heat pipe used in this simulation are shown in (table 1), with two heat sources (15 Watts and 15 Watts) in the evaporator section that separates by the adiabatic section.

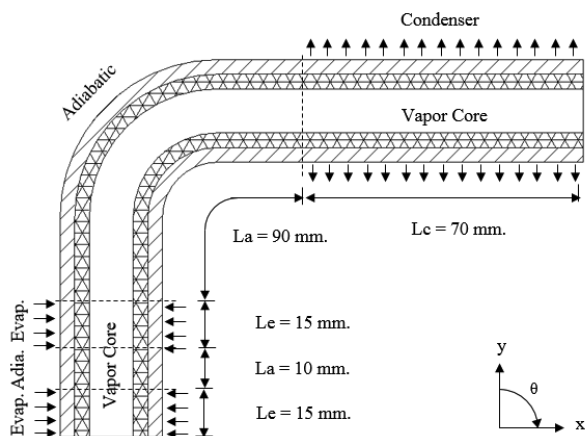


Figure 3 The schematic diagram of the heat pipe and dimension in this simulation.

Table 1 The specifications of bend heat pipe that used in this simulation.

Parameter	Value
Wall Material	Copper
Wick	Screen
Porosity	0.57
Permeability	$1.5 \times 10^{-9} \text{ m}^2$
k_{eff}	1.965 W/mK
Working Fluid	Water
Le, La, Lc	40, 90, 70 mm
Rv, Rw, Ro	2, 2.66, 3 mm.
Bending Angle	90 °
$Q_{\text{input}}, Q_{\text{output}}$	30 W

1. Pressure profile

(Figure 4) shows the pressure distributions along the heat pipe in vapor core. The pressure distribution was calculated from the continuity equations, the momentum equations, and the boundary conditions. The vapor pressure in the vapor core was constant at 20.51 kPa that was equal to the saturated pressure at the operating temperature along the heat pipe. From the results, it was shown that the pressure gradient in the vapor core was very small, because the viscosity of vapor is low. And it was founded that the pressure profile trends are in good agreement with the simulation results from N. Thuchayapong¹ that the vapor pressure in vapor core are constant along the heat pipe and equal to the saturated pressure at the operating temperature.

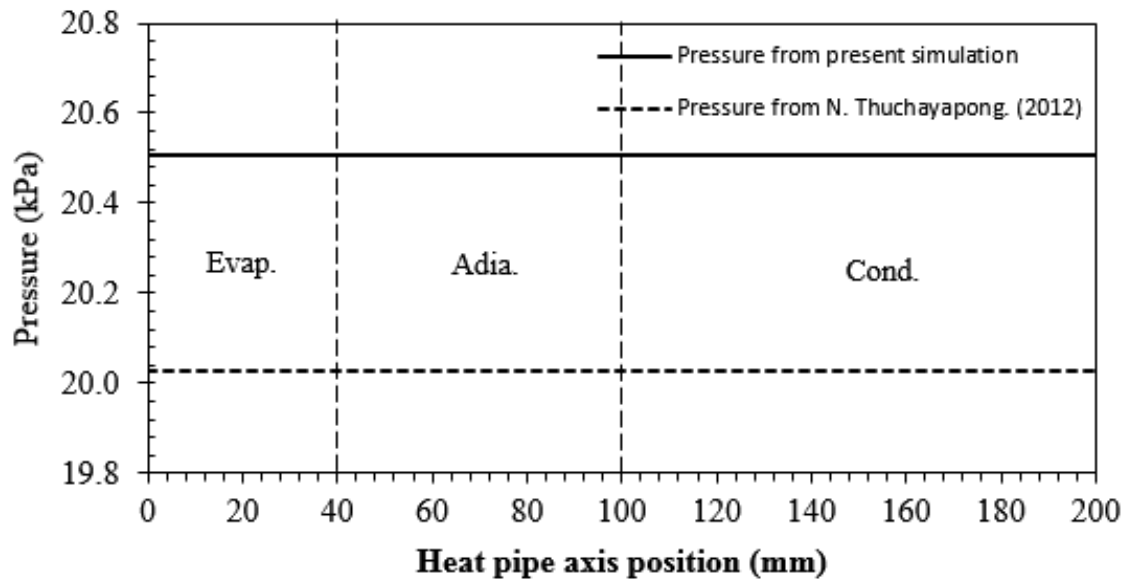


Figure 4 The vapor pressure along the heat pipe.

2. Velocity profile

The average axial velocity of vapor in the vapor core is shown in (Figure 5). The average axial velocity of vapor in the vapor core was calculated from the continuity equations, the momentum equations, and the boundary conditions. The vapor velocity increases from 0 to 7.17 m/s and 7.17 to 14.34 m/s from the end of the evaporator section to the interface between the evaporator and the adiabatic section because of increasing vapor mass from the evaporation of working fluid. The vapor velocity is constant in the adiabatic section because this section doesn't have heat input and output and decreases in the condenser section from 14.34 to 0 m/s

because of decreasing vapor mass from the condensation of working fluid. The vapor velocity at the end of the evaporator section increase quickly from 0 to 7.17 m/s in 15 mm, because the evaporation rate is in proportion to the capillary pressure. But it decrease linearly in the condenser section, because the condensation rate at the liquid-vapor interface in this section is constant at the liquid-vapor interface. It was founded that, the velocity profile trends are in good agreement with the simulation results from N. Thuchayapong¹ that the axial vapor velocity is increased in the evaporator section, constant in the adiabatic section and decrease in the condenser section.

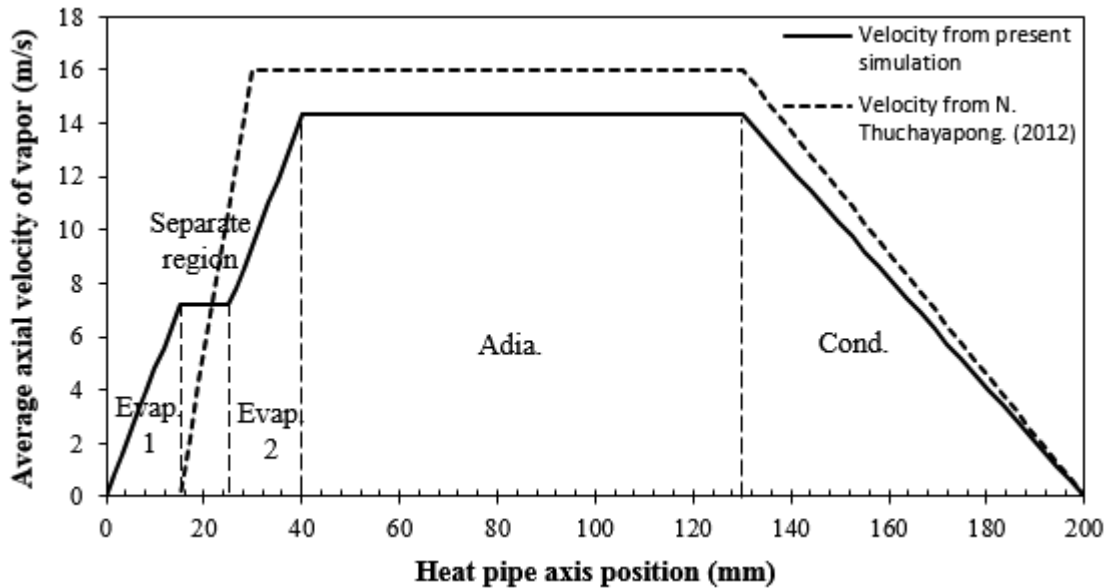


Figure 5 The average axial velocity of vapor along the heat pipe.

Conclusion

The vapor pressure in the vapor core are constant along the heat pipe and equal to the saturated pressure at the operating temperature. Axial vapor velocity increases in the evaporator section, is constant in the adiabatic section and decrease in the condenser section. This simulation was compared with data from from N. Thuchayapong, (2012) and in good agreement.

Acknowledgement

The authors gratefully acknowledge the Chiang Mai University Ph.D. Program (contract number PHD/006/2556) for funding this research.

References

- [1] N. Thuchayapong, Effect of tube bending on heat transfer characteristics of miniature heat pipe with sintered porous media,, 2012, Chiang Mai University, Thailand.
- [2] N. Thuchayapong, P. Terdtoon, P. Sakulchangsattajai, Simulation of Heat Pipe Performance by Using Finite Element Method, International Conference on Science, Technology and Innovation for Sustainable Well-Being (STISWB), 23-24 July 2009, Mahasarakham University, Thailand.
- [3] N. Thuchayapong, A. Nakano, P. Sakulchangsattajai, and P. Terdtoon, Effect of capillary pressure on performance of a heat pipe: Numerical approach with FEM, Applied Thermal Engineering, 32, January 2012, 93-99.
- [4] K.A.R. Ismail, M.A. Zanardi, A steady-state model for heat pipes of circular orrectangular cross-sections, Appl. Therm. Eng. 1996; 16 (8-9) 753-767.
- [5] S.V. Patankar, Numerical Heat Transfer and Fluid Flow. Hemisphere, New York, 1980.